PROCEEDINGS OF SCIENCE

DESY 11-025, FTUAM-11-37

Towards Four-Flavour Dynamical Simulations

Gregorio Herdoiza*
NIC, DESY
Platanenallee 6, 15738 Zeuthen, Germany
and
Departamento de Física Teórica and Instituto de Física Teórica UAM/CSIC
Universidad Autónoma de Madrid, Cantoblanco 28049 Madrid, Spain
E-mail: Gregorio.Herdoiza@desy.de

The inclusion of physical effects from sea quarks has been one of the main advances in lattice QCD simulations over the last few years. We report on recent studies with four flavours of dynamical quarks and address some of the potential issues arising in this new setup. First results for physical observables in the light, strange and charm sectors are presented together with the status of dedicated simulations to perform the non-perturbative renormalisation in mass-independent schemes.

The XXVIII International Symposium on Lattice Field Theory, Lattice2010
June 14-19, 2010
Villasimius, Italy

*Speaker.

PoS(Lattice 2010)010

Introduction

Non-perturbative studies of QCD on the lattice are steadily approaching a stage in which all systematic uncertainties present in the numerical calculations can be reliably estimated. A major advance during last decade has been to surpass the quenched approximation by the inclusion of sea quark effects. Dynamical simulations with $N_{\rm f} = 2$ flavours of mass-degenerate up and down sea quarks and $N_{\rm f} = 2+1$ calculations where the strange quark is also incorporated are currently being performed. For reviews on the status of these dynamical simulations at this and other recent lattice conferences, we refer to [1 – 4]. Investigations about the difficulties encountered in simulating at small values of the lattice spacing are reviewed in [5].

The Appelquist-Carazzone theorem [6] describes the decoupling of heavy particles at small momentum transfer. Loop effects from charm quarks should indeed be suppressed with respect to those of the other lighter sea quarks. At large momentum transfer charm quarks become active and physical processes could depend in a non-negligible way on charm loop effects. The renormalisation group running of renormalised quantities depends on the number of active flavours. In a mass-independent scheme, a matching between theories differing by the number of flavours is performed at a scale around the threshold quark mass above which this quark becomes active. For energy scales ranging between the charm and the bottom quark masses it is important to incorporate the effects of the active charm in the non-perturbative running with $N_{\rm f} = 4$ massless quarks. When considering renormalisation group invariant quantities, it is appropriate to opt for a realistic setup in which the physical charm-loop effects are included together with those of the lighter u, d and s sea quarks. These $N_{\rm f} = 2+1+1$ simulations allow to explore the effect of dynamical charm on hadron masses and matrix elements, thus removing this so far uncontrolled systematic effect.
Incorporating a charm quark in dynamical simulations can however introduce potential difficulties.

- The values of the inverse lattice spacing currently in use are not considerably larger than the charm quark mass m_c. Lattice artefacts proportional to m_c are thus in general significant, as it is well known from the study of observables involving charm quarks in the valence sector. In $N_{\rm f} = 2+1+1$ simulations, cutoff effects of this kind, but this time stemming from the fermionic determinant, can potentially affect all observables, even those without valence charm quarks. An explicit control of the size of cutoff effects in quantities that can be measured accurately – such as light-quark observables – in the presence of dynamical charm-loops can allow to address this issue.

- Dynamical simulations aim at setting the sea quark masses as close as possible to their physical values through the use of appropriate hadronic observables. In the $N_{\rm f} = 2+1+1$ case, the amount on computing resources dedicated to the tuning of the quark masses can be fairly large. It is therefore legitimate to wonder whether the tuning effort is prohibitive.

- Finally, the use of a mass-independent renormalisation scheme implies that dedicated simulations with $N_{\rm f} = 4$ massless, or nearly massless, quarks need to be considered. We remark that a similar effort is also needed in three-flavour simulations.

In the following, we will address these three issues based on recent four-flavour calculations.

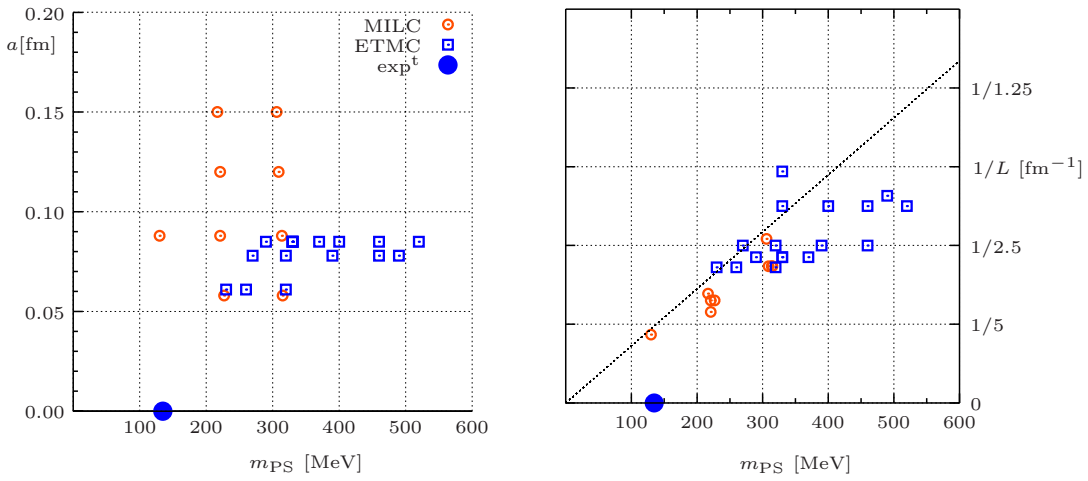

Figure 1: Parameter space of dynamical simulations with $N_f = 2+1+1$ flavours by MILC and ETMC. Simulation points (a) in the lattice spacing a and light pseudoscalar mass m_{PS} planes and (b) in the inverse lattice size $1/L$ and m_{PS} planes are considered. The oblique dotted line refers to the line of constant $m_{PS}L = 3.5$. The physical point is indicated by the blue circle.

1. $N_f = 2+1+1$ Simulations : Light-Quark Sector

In this section we review the recent $N_f = 2+1+1$ simulations by MILC and ETMC. A particular attention is given to the continuum-limit scaling of light-quark observables to identify potentially large cutoff effects due to the heavy mass m_c in the sea sector.

1.1 MILC Studies with HISQ Quarks

Simulation Setup. The MILC collaboration [7, 8] is producing ensembles with $N_f = 2+1+1$ flavours of highly improved staggered quarks (HISQ) [9]. In the gauge sector a tadpole-improved one-loop-Symanzik-improved action is used. The gauge action includes the effects of the quark loops in the one-loop coefficients. The HISQ action differs from the asqtad action used in the $N_f = 2+1$ simulations [10] by further smearing of the gauge links entering in the covariant derivative. HISQ quarks also include the Naik term, i.e. a third-nearest-neighbour coupling, with a mass-dependent correction to the tree-level improvement of the charm-quark dispersion relation. While being computationally more expensive than asqtad, the HISQ action is expected to reduce taste symmetry violations through the use of highly smeared links. For information about the lattice action and the algorithm, such as the modification of the guiding Hamiltonian to avoid large fluctuations in the fermion force, we refer to [7].

MILC ensembles cover four values of the lattice spacing, $a \approx \{0.06, 0.09, 0.12, 0.15\}$ fm. The light pseudoscalar meson mass m_{PS} varies from 315 MeV down to the physical point. The simulation at the physical pion mass is performed at a lattice spacing $a \approx 0.09$ fm and is in progress. The lattice size ranges between 2.4 and 5.5 fm and satisfies the condition $m_{PS}L > 3.5$. The red circles in Fig. 1 illustrate the status of the MILC $N_f = 2+1+1$ program [8]. Finalised ensembles include more than 5000 molecular dynamic units, with trajectory length ranging between 1.0 and 1.5 [7].

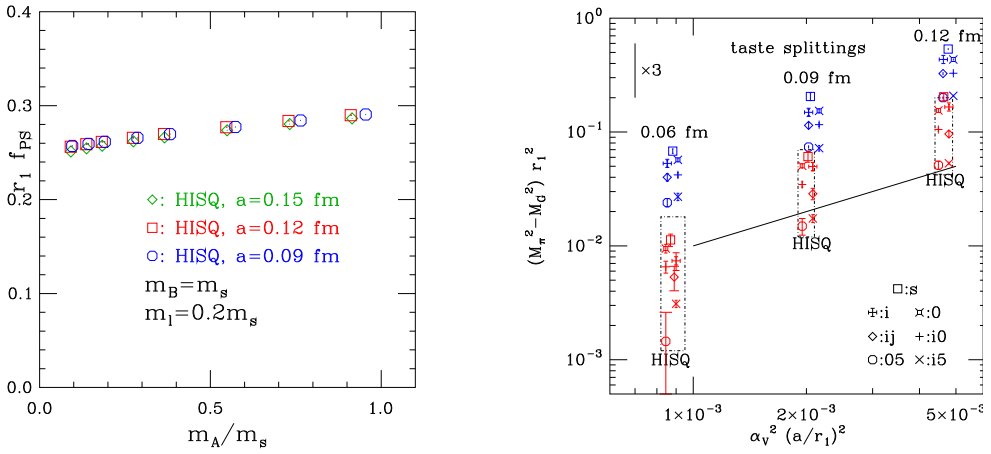

(a) (b)

Figure 2: Continuum-limit scaling studies by MILC. (a) Pseudoscalar meson decay constant $f_{\rm PS}$ in units of the scale r_1 as a function of the light-quark mass m_A (normalised by the strange quark mass m_s).The pseudoscalar meson is composed of the valence quark masses m_A and m_B, the latter being fixed to $m_B = m_s$. The unitary point corresponds to $m_A/m_s = 0.2$ in the x-axis. Small lattice artifacts are observed in the considered range of lattice spacings. (b) Continuum-limit scaling of the taste splittings of pions. $M_{\rm G}$ stands the mass of the lightest (Goldstone) pion, while M_π refers to the remaining pion masses, organised by taste structure. A reduction of taste symmetry breaking is observed when moving from the $N_{\rm f} = 2+1$ asqtad action (blue symbols) to the $N_{\rm f} = 2+1+1$ HISQ one (red symbols).

Continuum-Limit Scaling. As shown in Fig. 1, MILC has generated ensembles with fixed pseudoscalar mass $m_{\rm PS}$ and lattice size L at four values of the lattice spacing. Such a setup is well suited for a continuum-limit scaling [7]. The values of the bare charm quark mass in lattice units vary from $am_c \approx 0.44$ at $a \approx 0.09\,$fm up to $am_c \approx 0.84$ at the coarser lattice spacing $a \approx 0.15\,$fm [7, 8]. It is instructive to examine if values of $am_c \lesssim 1$ induce large lattice artefacts in light-quark observables. The case of the pseudoscalar meson decay constant $f_{\rm PS}$ is shown in Fig. 2(a). The scale r_1 [11] is used to relate different lattice spacings. It is determined in a similar way to the Sommer scale r_0 [12], from the force between static quarks. Fig. 2(a) shows no evidences for large cut-off effects in $r_1 f_{\rm PS}$. Furthermore, compared to $N_{\rm f} = 2+1$ asqtad data, a reduction of lattice artefacts is observed for $N_{\rm f} = 2+1+1$ HISQ ensembles [7]. Similar effects are observed for other quantities such as the vector meson mass, the nucleon mass or the topological susceptibility [7, 8].

Taste Symmetry Breaking. Each staggered fermion field generates four degrees of freedom, the so called tastes. In a theory with $N_{\rm f} = 4$ mass-degenerate quarks, these four tastes can be interpreted as quark flavours. In the $N_{\rm f} = 2+1+1$ case, where the sea quark masses satisfy, $m_u = m_d < m_s < m_c$, a "rooting procedure" is applied to the fermionic determinant in order to eliminate the contribution of unwanted tastes. As a result, locality and unitarity of the theory do not hold at non-zero lattice spacing [10]. Assessing the validity of the approach once the continuum-limit is taken has triggered a number of studies (see [10] and references therein for an account on the rooting issue). With stag-

gered quarks, mesons appear in 16 species differing by their taste content. At finite lattice spacing, the breaking of taste symmetry introduces mass-splittings among these mesons. When taking the continuum limit, mass-splittings among non-singlet mesons are expected to vanish. These splittings are largest for the pion system and typically amount for bigger discretisation effects than other more standard (i.e. not related to taste symmetry breaking) lattice artifacts. Determining the size of taste breaking effects is therefore an important check of the setup. Fig. 2(b) shows the lattice spacing dependence of the pion taste splittings. At fixed lattice spacing a significant reduction (of around a factor of three) in the size of the taste splittings is observed when switching from asqtad to HISQ. Since the generation of $N_f = 2+1+1$ ensembles is in progress [8], first physical results from MILC are expected to appear in the near future.

1.2 ETMC Studies with Wilson twisted mass (Wtm) Fermions

Simulation Setup. The ETM collaboration is performing simulations with $N_f = 2+1+1$ flavours of Wilson twisted mass (Wtm) fermions [13]. [1] The Iwasaki action [15] is used in the gauge sector. This choice is driven by considerations on the phase structure of Wilson fermions. With respect to the tree-level Symanzik-improved gauge action [16], which was used in $N_f = 2$ simulations [17, 18], ETMC observes that in the $N_f = 2+1+1$ case, the Iwasaki action provides a smoother variation of observables around the critical mass [13, 19]. The fermionic action is composed of two doublets of Wtm fermions. Note that the use of an even number of flavours, e.g. $N_f = 2+1+1$, is a natural choice for Wtm fermions. The action for the mass-degenerate light doublet (u, d) reads [20, 21]

$$S_\ell \;=\; a^4 \sum_x \{\bar{\chi}_\ell(x)\,[D_{\rm W}[U] + m_{0,l} + i\mu_\ell \gamma_5 \tau_3]\,\chi_\ell(x)\}\;, \tag{1.1}$$

where $\chi_\ell = (\chi_u, \chi_d)$, D_W is the massless Wilson-Dirac operator, $m_{0,l}$ is the untwisted bare quark mass, μ_ℓ is the bare twisted light quark mass and τ_3 is the Pauli matrix acting in flavour space. For the heavier non-degenerate (c, s) doublet the action takes the following form [22, 23]

$$S_h \;=\; a^4 \sum_x \{\bar{\chi}_h(x)\,[D_{\rm W}[U] + m_{0,h} + i\mu_\sigma \gamma_5 \tau_1 + \mu_\delta \tau_3]\,\chi_h(x)\}\;, \tag{1.2}$$

where $\chi_h = (\chi_c, \chi_s)$, $m_{0,h}$ is the untwisted quark mass, μ_σ the twisted mass – the twist is along the τ_1 direction – and μ_δ the mass splitting along the τ_3 direction. The bare mass parameters μ_σ and μ_δ are related to the renormalised strange and charm quark masses [22]:

$$(m_s)_{\rm R} = Z_{\rm P}^{-1}\,(\mu_\sigma - Z_{\rm P}/Z_{\rm S}\,\mu_\delta)\,, \qquad (m_c)_{\rm R} = Z_{\rm P}^{-1}\,(\mu_\sigma + Z_{\rm P}/Z_{\rm S}\,\mu_\delta)\,,$$

where $Z_{\rm P}$ and $Z_{\rm S}$ are the renormalisation constants of the pseudoscalar and scalar non-singlet quark densities, respectively, computed in the massless $N_f = 4$ standard Wilson theory. The $\mathcal{O}(a)$ improvement of physical observables is obtained by working at maximal twist [21, 22]. This is achieved by imposing [14] $am_{0,l} = am_{0,h} \equiv 1/2\kappa - 4$ and by setting $\kappa = \kappa_{\rm crit}$ through the tuning of the light PCAC quark mass to zero at each set of values $\{\mu_\ell, \mu_\sigma, \mu_\delta\}$. For more information about the lattice setup, the tuning to maximal twist and the algorithm we refer to [13].

ETMC ensembles include three values of the lattice spacing , $a \approx \{0.06, 0.08, 0.09\}$ fm and lattice extents ranging from 1.9 to 2.7 fm. The light pseudoscalar mass $m_{\rm PS}$ varies from 520 MeV

[1] This setup was first explored in [14].

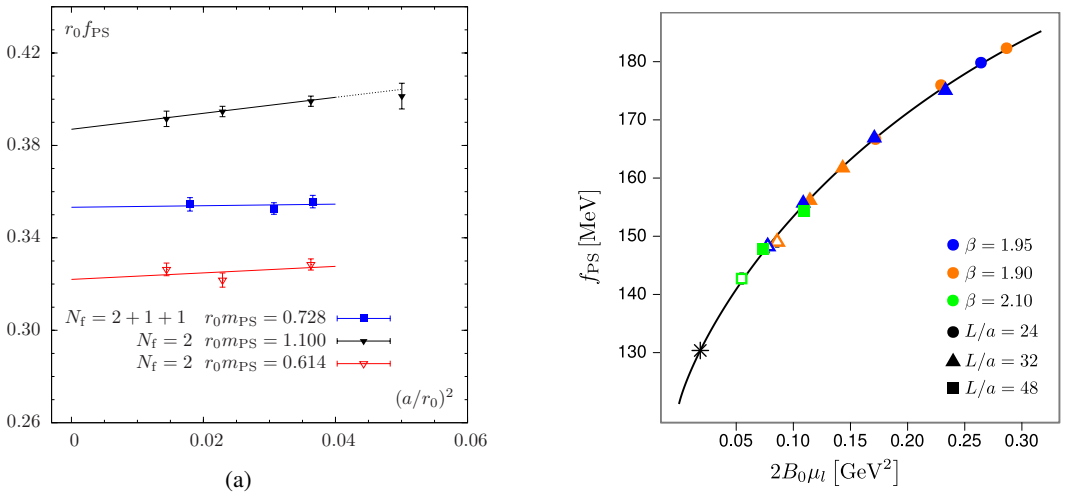

Figure 3: (a) ETMC study of the continuum-limit scaling of the light pseudoscalar meson decay constant $f_{\rm PS}$ in units of the Sommer scale r_0, at fixed reference values of $m_{\rm PS}$. Mild cutoff effects are observed and a comparison to $N_{\rm f}=2$ ETMC data indicates a similar scaling behaviour for $r_0 f_{\rm PS}$. (b) $f_{\rm PS}$ as a function of the light quark mass (B_0 is the LO χPT LEC). A continuum NLO SU(2) χPT fit to data from three values of the lattice spacing, $a \approx \{0.06,\ 0.08,\ 0.09\}$ fm, was used to estimate systematic effects in the determination of the LECs [24]. The experimental value pion decay constant (black star) was used to set the scale.

down to 230 MeV. For each point, the largest lattice size satisfies $m_{\rm PS} L \gtrsim 3.5$. The blue squares in Fig. 1 illustrate the status of the ETMC $N_{\rm f}=2+1+1$ simulations [24]. Ensembles contain 5000 thermalised trajectories of length $\tau = 1$.

Continuum-Limit Scaling. The lattice spacing dependence of the charged pion decay constant $f_{\rm PS}$ is illustrated in Fig. 3(a). The scaling is consistent with the expected $\mathcal{O}(a)$ improvement. A comparison to the $N_{\rm f}=2$ case [25] is also shown. A good scaling behaviour with no signs of large cutoff effects due to the dynamical charm is observed in $f_{\rm PS}$, as well as in the nucleon mass [29]. The values of the bare charm quark mass in lattice units satisfy $am_c \lesssim 0.3$. As previously discussed, the physical effect from charm-loops should be small and suppressed with respect to that of the other lighter quarks. It is therefore expected that cutoff effects from dynamical charm-quarks appear as a correction to this small effect.

Physical Results in the Light Sector. The light-quark mass and the volume dependence of $m_{\rm PS}$ and $f_{\rm PS}$ have been studied by means of chiral perturbation theory (χPT). At next-to-leading order (NLO) in continuum SU(2) χPT [26], four low-energy constants (LEC), B_0, f_0, $\bar{l}_{3,4}$, contribute to the mass dependence of $m_{\rm PS}$ and $f_{\rm PS}$. Finite size effects (FSE) were corrected by the resummed Lüscher formulae combined with χPT [27]. Fig. 3(b) illustrates a χPT fit to $f_{\rm PS}$ for three values of the lattice spacing. The central values and statistical errors reported by ETMC [13, 24] have been determined from a fit to a single lattice spacing, $a \approx 0.08$ fm. Systematic effects can arise through lattice artifacts, FSE or higher order terms in χPT. Although a full account of sys-

tematic uncertainties is still missing, we refer to [13, 24] for a report on the current estimates. The resulting $N_f = 2+1+1$ determinations from χPT fits are $f_\pi/f_0 = 1.076(3)$, $\bar{l}_3 = 3.70(27)$, $\bar{l}_4 = 4.67(10)$ [13, 24]. A good agreement is observed when comparing these determinations to $N_f = 2$ ETMC results [25] and to other lattice calculations [28]. Studies of other light-quark observables, such as the nucleon and Δ masses [29] or nucleon matrix elements [30] were presented at this conference.

Isospin Breaking. The Wtm action breaks isospin at finite lattice spacing inducing a mass splitting between charged and neutral pions. This splitting is a lattice artifact which is expected to vanish in the continuum at a rate of $\mathcal{O}(a^2)$. In the $N_f = 2$ case, ETMC observed mild discretisation effects in the continuum-limit scaling of the charged pseudoscalar meson mass $m^{\pm}_{\rm PS}$ [25, 31] while significant cutoff effects were present in the mass splitting $m^0_{\rm PS} - m^{\pm}_{\rm PS}$ [25]. Recent studies [13], indicate that this splitting increases when increasing N_f from two to four.[2] In the expression $r_0^2((m^0_{\rm PS})^2 - (m^{\pm}_{\rm PS})^2) = c\,(a/r_0)^2$, the sign of the factor c is related to the type of scenario expected for the phase structure of Wilson fermions in the regime of small quark masses [32, 33]. When c is negative, it measures the strength of the first order phase transition [34–36]. The determination of the $m^0_{\rm PS}$ involves quark-disconnected contributions. Fig. 4(a) shows the scaling of the pion mass splitting for $N_f = 2$ and $N_f = 2+1+1$ ETMC simulations. The values of c are $c \approx -6$ in the $N_f = 2$ case and $c \approx -10$ in the $N_f = 2+1+1$ one. Besides the pion mass, isospin breaking cutoff effects can effect other observables. For $N_f = 2$ ensembles, large isospin breaking effects have been observed only in the neutral pion mass [25], in agreement with an analysis based on the Symanzik expansion [37, 38]. A similar scenario for isospin breaking cutoff effects is expected to hold in the $N_f = 2+1+1$ case. Explicit control of isospin breaking, in particular by performing the continuum extrapolation, is the appropriate way of addressing this issue. First analyses of the Δ baryon masses indicate that isospin breaking effects are negligible at the three values of the lattice spacing [29].

The breaking of isospin and parity can be described in Wilson twisted mass chiral perturbation theory (tmWχPT) [34–36]. The impact of $m^0_{\rm PS}$ in the volume [39] and quark-mass dependence [40] of the charged pion mass and decay constant has recently been studied in tmWχPT. The quality of the fits is reported to improve [39, 40] when including isospin breaking effects. For $N_f = 2$ data, the impact of these corrections on the determination of the light-quark mass was observed to be at most at the level of the fitting errors [31]. ETMC has planned a dedicated study on this issue in the $N_f = 2+1+1$ case.

2. Strange and Charm Sectors

Tuning Effort. The simulated quark masses are to be set as close as possible to their physical values. For the light (u, d) quarks this usually implies a chiral extrapolation though recent progress in the field goes precisely in the direction of simulating directly at the physical point [1]. The strange and charm quark masses are directly accessible on current lattices. Since a reliable estimate of the lattice spacing is only available a posteriori, setting m_s and m_c typically requires considering a set of values such that a small interpolation to the physical point can be performed. Such a procedure

[2] Note however that the gauge action changed between the $N_f = 2$ to $N_f = 2+1+1$ calculations.

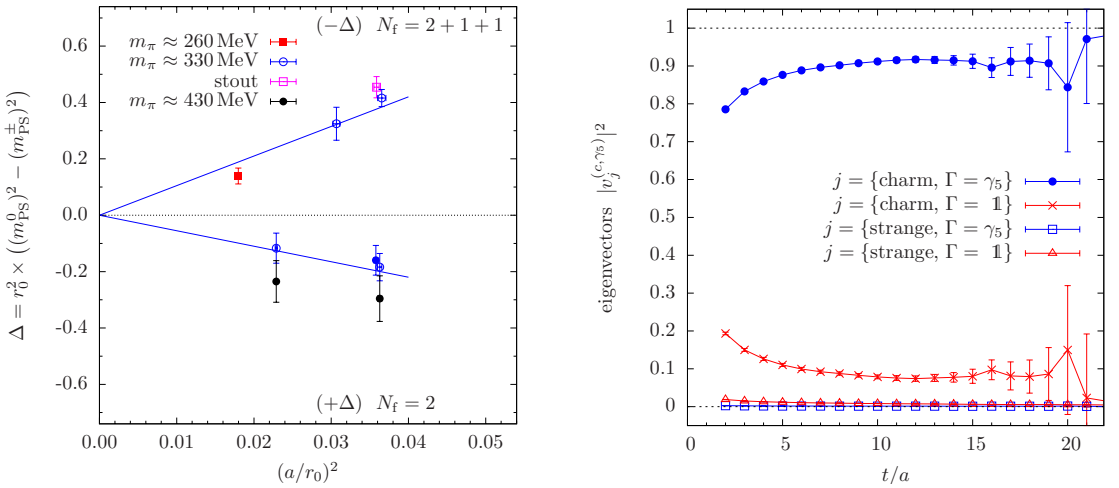

(a) (b)

Figure 4: (a) Continuum-limit scaling of the pion mass splitting Δ in units of r_0 for $N_f = 2+1+1$ and $N_f = 2$ flavours of twisted mass fermions. For a better visibility a global minus sign is given to the $N_f = 2+1+1$ data. The blue lines suggest the expected behaviour towards the continuum limit. An increase of isospin breaking effects are observed when increasing the number of dynamical flavours. The empty square refers to a $N_f = 2+1+1$ ensemble with one level of stout smearing presenting a similar mass splitting than a 'non-stout' ensemble. (b) Approximate flavour and parity content of an state extracted from solving the GEP at $a \approx 0.06$fm. The state is dominated by the D-meson quantum numbers.

is also required to address the non-negligible systematic effect associated to different ways of setting the scale on the lattice. The inclusion of a dynamical charm implies a further computational effort with respect to $N_f = 2+1$ simulations, due to the additional tuning of m_c. When aiming at an interpolation to the charm quark mass, an increase by roughly a factor of two in computing time is needed with respect to $N_f = 2+1$ calculations. The tuning effort depends on the sensitivity of the observables of interest to the quark mass and on the target accuracy one aims to achieve. Reweighting techniques can be useful to perform the small quark mass corrections in the strange and charm sectors (see [2] for a review). As discussed in Section 3, the non-perturbative renormalisation requires dedicated simulations with $N_f = 4$ mass-degenerate flavours. Hence, carrying out an $N_f = 2+1+1$ simulation program implies an overall increase in the computational effort with respect to the $N_f = 2$ and $N_f = 2+1$ cases. [3] Recent studies with four dynamical flavours also indicate that this additional effort is not a fundamental limitation.

To set m_s and m_c, MILC uses the physical values of $2m_K^2 - m_\pi^2$ and $(m_{\eta_c} + 3m_{J/\Psi})/4$, respectively. Quark-disconnected contributions are not included in the determination of the charmonium masses but recent studies [41] indicate that they should amount to a sub-percent effect on the spin-averaged mass. In the context of $N_f = 2+1$ simulations, QCDSF-UQKCD [42] is using an alternative method to set the strange quark mass. Rather than keeping the strange quark mass fixed when performing the light-quark mass extrapolation, it is the sum of the quark masses $m_u + m_d + m_s$ that is kept fixed. A mild dependence of singlet quantities is then observed when extrapolating data

[3] As mentioned in Section 3, we note that in the $N_f = 2+1$ case, dedicated simulations for non-perturbative renormalisation with $N_f = 3$ flavours should also be included in the overall computational cost.

from the SU(3) symmetric point towards the physical point.

ETMC Studies of Kaon and D-meson Masses. The twisted mass action (1.2) for the (c,s) doublet is non-diagonal in flavour space.[4] This induces, at finite lattice spacing, a mixing between strange and charm quarks. The breaking of flavour symmetry and parity imply that the identification of the D-meson state is not straightforward since its signal appears among other excited states at intermediate Euclidean time separations. The ground state is dominated by the Kaon and its identification is therefore unambiguous. Isolating the D-meson by resolving all the excited states above the Kaon would require large correlation matrices with high statistical precision. However, in the D-meson channel, the coupling to low-lying states allowed by mixing is a pure cut-off effect and should therefore be progressively suppressed towards the continuum limit. At finite lattice spacing, the D-meson state is expected to have a significant contribution to the signal in the appropriate correlation functions at intermediate time separations.

Based on this observation, ETMC has developed three methods to identify the D-meson state and to determine its mass [43, 44]. These methods rely on (i) solving a generalised eigenvalue problem (GEP), (ii) fitting the correlation matrix by a series of exponentials and (iii) enforcing flavour and parity restoration at finite lattice spacing. We refer to [43] for a detailed description of the different methods. Fig. 4(b) shows the approximate heavy flavour and parity contents of an excited state as determined from the GEP, i.e. method (i), suggesting that it is dominated by the quantum numbers of the D-meson state. Consistent results are found for the D-meson mass determined by means of the three methods [43, 44]. The restoration of parity and flavour symmetry can be monitored through the continuum-limit scaling of the elements of the correlation matrix from which the D-meson mass is extracted. A scaling study of the D-meson mass in the free theory has recently been reported in [45].

The status of the tuning of m_s and m_c in ETMC ensembles, through the use of $2m_K^2 - m_\pi^2$ and m_D, respectively, is shown in Figs. 5. The simulated points are in the neighbourhood of the physical points (black stars) with maximal deviations from the physical values of $m_{s,c}$ of the order of $\sim 20\%$. Further tuning runs aiming to interpolate $m_{s,c}$ to the physical point are currently being performed [24].

ETMC Studies of a Mixed Action with Osterwalder-Seiler (OS) Quarks. Precision studies of charm-quark observables with the action (1.2) is complicated by the presence of the c-s mixing discussed above. This problem is avoided in the valence sector by considering a mixed action setup[5] where the valence c and s quarks are introduced with a flavour diagonal action. Osterwalder-Seiler (OS) valence quarks [46] can be viewed as the building blocks of Wtm fermions at maximal twist. The OS action for an individual quark flavour q_f reads

$$S_{\rm OS} \;=\; \bar{q}_f(x)\left[\gamma_\mu\tilde{\nabla}_\mu - i\,r_f\,\gamma_5\left(-\frac{a}{2}\nabla^*_\mu\nabla_\mu + m_{\rm cr}\right) + \mu_f\right] q_f(x)\,,$$

where r_f (here $|r_f| = 1$) is the Wilson parameter and $m_{\rm cr}$ the critical mass. By combining two flavours of OS quarks with opposite signs of r_f, e.g. $r_2 = -r_1$, the action of a doublet of maximally

[4] This is most easily seen when rewriting the action in eq. (1.2) in the physical quark basis.

[5] A mixed action consists in employing different discretisations of the Dirac operator for sea and valence quarks. It is thus possible to restore in the valence sector a symmetry which is broken in the sea sector.

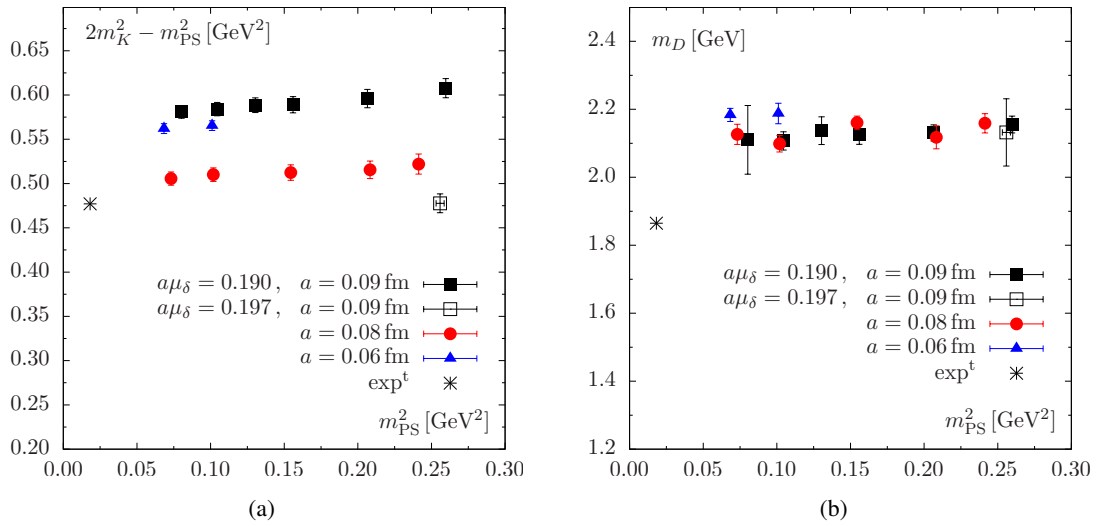

Figure 5: Status of the tuning of (a) the strange and (b) the charm quark mass in $N_f = 2+1+1$ ETMC ensembles with $a \approx \{0.06, 0.08, 0.09\}$ fm. The physical point is denoted by the black star.

twisted mass fermions of mass $\mu_f = \mu_1 = \mu_2$ can be recovered. Note that the constraint $\mu_1 = \mu_2$ is not necessary for valence quarks whereas it is crucial in the sea sector in order to guarantee the reality of the fermionic determinant. In fact, the determinant of the one-flavour OS lattice Dirac operator is in general complex. The benefits of the OS action are that $\mathcal{O}(a)$ improved physical observables [22] can be achieved by using the same estimates of m_{cr} than in the Wtm case thus avoiding further tuning effort. OS and Wtm fermions coincide with Wilson fermions in the massless limit and therefore share the same renormalisation factors. This simplifies the matching of sea and valence quark masses in the context of a mixed action. Finally, the OS action being flavour diagonal, it is a natural choice for avoiding the previously discussed strange and charm mixing in the valence sector.

A similar mixed action with $N_f = 2$ Wtm sea fermions and OS valence quarks was employed by ETMC [47]. The motivation for such a setup is to determine the Kaon bag parameter B_K with Wilson-type fermions by simultaneously preserving $\mathcal{O}(a)$ improvement and absence of wrong chirality operator mixings [22, 47, 48]. The mixed action OS mesons were constructed by using the same sign of r_f, $r_1 = r_2$, in the two quark propagators, while the unitary mesons had opposite signs, $r_1 = -r_2$. Fig. 6(a) shows the continuum limit scaling of m_K^2 for the unitary and mixed action mesons [47]. The scaling behaviour is consistent with $\mathcal{O}(a)$ improvement and unitarity violations in the mixed action are observed to vanish in the continuum limit. Significantly larger cut-off effects are reported in Fig. 6(a) when the meson is built of quarks with the same signs of r_f (red squares). A good scaling behaviour is observed instead in the case of f_K [47]. For the meson with valence quarks having $r_1 = -r_2$, the scaling of both m_K^2 (blue circles) and f_K show only moderate $\mathcal{O}(a^2)$ lattice artifacts [47].

When considering the $N_f = 2+1+1$ case, a mixed action can be employed in the strange and charm sectors. The mixed action Kaon and D-meson include s and c sea quark effects arising the action in eq. (1.2) while OS quarks, with $r_1 = -r_2$, are used in the valence sector. Fig. 6(b) compares unitary and mixed action determinations of f_K [49] once the sea and valence strange

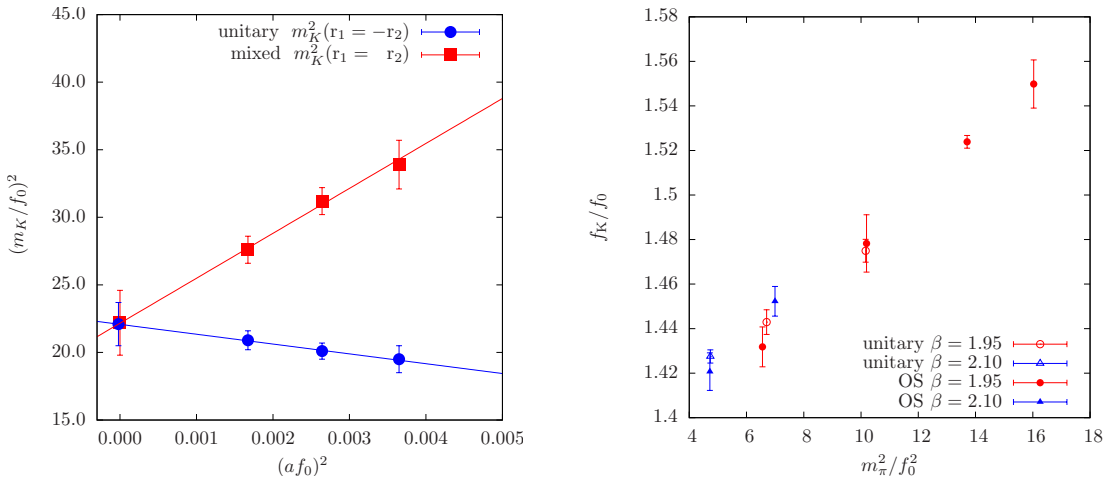

(a) (b)

Figure 6: ETMC studies of mixed actions with OS valence quarks. (a) Continuum-limit scaling of m_K^2 for unitary and mixed action Kaons in $N_f = 2$ ensembles. The chirally extrapolated pseudoscalar decay constant f_0 is used as scaling variable. The restoration unitarity is observed in the continuum limit. (b) Unitary and mixed action f_K from $N_f = 2+1+1$ ensembles with $a \approx 0.06$ and 0.08 fm. With the current accuracy, both unitarity violations and more standard discretisation effects are found to be small for this quantity.

quark masses have been matched via the Kaon mass. No signs of large unitarity violations are observed in this quantity. Additionally, the values of f_K from two lattice spacings, $a \approx 0.06$ and 0.08 fm, agree within errors, suggesting that discretisation effects are small.

An SU(2) χPT fit together with an interpolation in the valence sector to the experimental value of $2m_K^2 - m_\pi^2$, provides preliminary estimates of $f_K = 160(2)$ MeV and $f_K/f_\pi = 1.224(13)$ [49], where only statistical errors are quoted.[6] These $N_f = 2+1+1$ estimates are compatible with other recent results from $N_f = 2$ and $N_f = 2+1$ calculations [1, 28]. First determinations of the pseudoscalar meson masses and decay constants in the charm sector [49] and of the low-lying baryon spectrum [29] were reported at this conference.

3. Non-Perturbative Renormalisation

Many observables, including fundamental parameters of QCD such as the strong coupling constant or the quark masses, require a renormalisation procedure. On the lattice, the removal of UV divergences can in principle be performed by means of lattice perturbation theory. However, in practise, the truncation errors can be large due to the poor convergence of the series and to difficulties in determining higher order terms. Non-perturbative renormalisation allows to overcome these problems.

The absence of mass-dependence in the anomalous dimensions entering in the renormalisation group equations is guaranteed in mass-independent renormalisation schemes [50]. In lattice computations, this implies that the effects of all active quark flavours need to be incorporated and that the chiral limit of each of the quark masses has to be taken. When aiming at the renormalisation

[6] As in the light sector, the experimental value of f_π is used to set the scale.

of scale-dependent observables determined from $N_f = 2+1$ and $N_f = 2+1+1$ simulations, the chiral limit of the strange and charm quark masses has to be taken during renormalisation implying that dedicated simulations with $N_f = 3$ and $N_f = 4$ degenerate flavours, respectively, need to be performed. Keeping the quark masses fixed to their physical values would introduce a systematic effect at the level of renormalisation. Due to its large mass, the charm quark would tend to decouple from the dynamics while, in a mass-independent scheme, it should behave as an active quark.

The non-perturbative renormalisation schemes currently in use are the Schrödinger Functional (SF) [51] and the RI-MOM [52] schemes. We refer to [53] for a review on recent developments on these schemes and variants of them. In the SF it is possible to work directly with massless quarks while a chiral extrapolation has to be performed in the case of RI-MOM. Several groups have recently performed dynamical simulations with $N_f = 3$ and $N_f = 4$ degenerate flavours.

The running of the coupling [54] and of the quark mass [55] with $N_f = 3$ flavours has been determined through the step-scaling function in the SF scheme by PACS-CS using the Iwasaki gauge action and non-perturbatively $\mathcal{O}(a)$ improved Wilson fermions. Dedicated $N_f = 3$ simulations have been performed by BMW to renormalise the quark mass in the RI-MOM scheme [56] with the tree-level improved Symanzik gauge action and tree-level improved Wilson fermions coupled to gauge links with two levels of HEX smearing.

In the four-flavour case, ETMC is currently generating ensembles with two degenerate doublets of Wtm fermions [7] and the Iwasaki gauge action to perform the renormalisation in RI-MOM scheme [57]. In these $N_f = 4$ simulations, the PCAC quark mass, $m_{\rm PCAC}$, does not show a sufficiently smooth dependence on the untwisted quark mass $m_{0,l}$ around its critical value, for $a \gtrsim 0.08\,\mathrm{fm}$ and a twisted mass $\mu_\ell \approx 0.4 m_s$. Indeed, for simulations close to maximal twist, i.e. $m_{\rm PCAC} \approx 0$, the integrated autocorrelation time of $m_{\rm PCAC}$ significantly grows. Simulating at maximal twist would therefore require fairly long runs to reliably control the value and error of $m_{\rm PCAC}$. The stability of the simulations improves when working out of maximal twist, i.e at non vanishing values of both the standard (untwisted) mass and the twisted mass parameter. In this case, the renormalised quark mass is given by the polar mass, $\widehat{M} = Z_{\rm P}^{-1}\sqrt{Z_{\rm A}^2 m_{\rm PCAC}^2 + \mu_\ell^2}$, which should eventually be extrapolated to the chiral limit. The $\mathcal{O}(a)$ improvement of the renormalisation factors is achieved by averaging estimators from simulations with equal $\widehat{M}$ but opposite values of $m_{\rm PCAC}/\mu_\ell$ [57]. Fig. 7(a) shows the sea quark mass dependence of quark-bilinear renormalisation factors from a preliminary analysis at $a \approx 0.08\,\mathrm{fm}$. The mild dependence on the sea quark mass is in line with ETMC studies in the two-flavour case [58].

The running up to high energy scales of the QCD coupling with $N_f = 4$ flavours has been recently determined non-perturbatively in the SF scheme by two groups. The study by the ALPHA collaboration [59, 60] uses the Wilson plaquette gauge action and non-perturbatively $\mathcal{O}(a)$ improved Wilson fermions. Given the current statistical precision, cutoff effects in the step-scaling function are observed to be small at the two finer lattice spacings. Fig. 7(b) shows the non-perturbative running of the coupling and a comparison to perturbation theory. The observed deviations from perturbation theory at low-energies (vertical dashed line), is a warning about the use of perturbation theory in a regime where the coupling is not sufficiently weak. The running of the coupling is also being studied by S. Sint and P. Pérez Rubio [61] using the plaquette gauge action

[7] The fermionic action for each of the doublets corresponds to eq. (1.1).

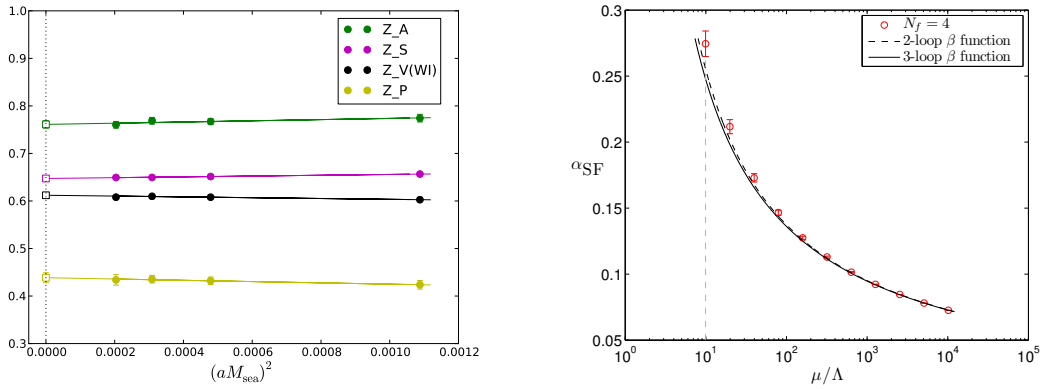

(a) (b)

Figure 7: (a) Sea quark mass dependence of quark bilinear renormalisation factors from $N_{\rm f} = 4$ ETMC calculations in the RI-MOM scheme at $a \approx 0.08\,$fm. (b) Non-perturbative running of the $N_{\rm f} = 4$ QCD coupling in the SF scheme as determined by the ALPHA collaboration. A comparison to perturbation theory is shown.

and a single staggered fermion field, corresponding to four flavours of massless quarks. Two regularisations differing by the time extent, $T = L \pm a$, are used to estimate systematic effects due to lattice artifacts. Indeed, in this way, non-negligible cutoff effects are identified in the step-scaling function [61]. It is interesting to note that these two studies of the $N_{\rm f} = 4$ running coupling can be used to check the universality of the step-scaling function. A natural extension of these investigations is the determination of the Λ parameter, which requires the input of a physical quantity determined from $N_{\rm f} = 2+1+1$ simulations.

Conclusions

Several studies have recently been devoted to lattice QCD simulations with four dynamical flavours. First physical results from observables in the light, strange and charm sectors have been presented at this conference. As an important check of this new simulation setup, the study of light-quark observables, such as the light pseudoscalar decay constant or the nucleon mass, revealed a good continuum-limit scaling behaviour, with no clear evidence of large cutoff effects coming from the heavy charm quark in the sea. The overall computational cost of the four flavour simulation program is larger than that of $N_{\rm f} = 2$ or $N_{\rm f} = 2+1$ calculations due to further tuning effort of the quark masses. Furthermore, dedicated simulations for non-perturbative renormalisation need to be performed. The fact that several lattice groups have already started these calculations clearly indicates that such a computational effort is not a strong limitation to proceed with four-flavour QCD simulations. Studies of the continuum-limit scaling of observables containing valence charm quarks and of quantities requiring renormalisation are among the open questions which still need to be addressed in this novel setup.

Acknowledgements

I thank P. Dimopoulos, R. Frezzotti, K. Jansen and C. Urbach for very useful suggestions and dis-

cussions and for comments on this manuscript. I wish to thank P. Boyle, T.W. Chiu, N. Christ, P. Dimopoulos, V. Drach, F. Farchioni, R. Frezzotti, E. García Ramos, S. Gottlieb, C. Hoelbling, K. Jansen, C. Lang, V. Lubicz, C. McNeile, C. Michael, I. Montvay, D. Palao, P. Pérez Rubio, D. Pleiter, S. Reker, D. Renner, G.C. Rossi, F. Sanfilippo, S. Sharpe, A. Shindler, S. Sint, R. Sommer, C. Tarantino, D. Toussaint, C. Urbach, M. Wagner, U. Wenger and all my colleagues from ETMC for help in preparing this work.

References

[1] C. Hoelbling, PoS **LATTICE 2010** (2010) 011. [arXiv:1102.0410].

[2] C. Jung, PoS **LAT2009** (2009) 002. [arXiv:1001.0941].

[3] E. E. Scholz, PoS **LAT2009** (2009) 005. [arXiv:0911.2191].

[4] K. Jansen, PoS **LATTICE 2008** (2008) 010. [arXiv:0810.5634].

[5] M. Lüscher, PoS **LATTICE 2010** (2010) 015. [arXiv:1009.5877].

[6] T. Appelquist, J. Carazzone, Phys. Rev. **D11** (1975) 2856.

[7] **MILC**, A. Bazavov *et al.*, Phys. Rev. **D82** (2010) 074501. [arXiv:1004.0342].

[8] **MILC**, A. Bazavov *et al.*, PoS **LATTICE 2010** 320. [arXiv:1012.1265].

[9] **HPQCD-UKQCD**, E. Follana *et al.*, Phys. Rev. **D75** (2007) 054502. [hep-lat/0610092].

[10] **MILC**, A. Bazavov *et al.*, Rev. Mod. Phys. **82**, 1349-1417 (2010). [arXiv:0903.3598].

[11] C. W. Bernard *et al.*, Phys. Rev. **D62** (2000) 034503. [hep-lat/0002028].

[12] R. Sommer, Nucl. Phys. **B411** (1994) 839-854. [hep-lat/9310022].

[13] **ETMC**, R. Baron *et al.*, JHEP **1006** (2010) 111. [arXiv:1004.5284].

[14] T. Chiarappa *et al.*, Eur. Phys. J. **C50** (2007) 373-383. [hep-lat/0606011].

[15] Y. Iwasaki, Nucl. Phys. **B258**, 141-156 (1985).

[16] P. Weisz, Nucl. Phys. **B212** (1983) 1.

[17] **ETMC**, Ph. Boucaud *et al.*, Phys. Lett. **B650**, 304 (2007), [arXiv:hep-lat/0701012].

[18] **ETMC**, Ph. Boucaud *et al.*, Comput. Phys. Commun. **179** (2008) 695, [arXiv:0803.0224].

[19] F. Farchioni *et al.*, Eur. Phys. J. C **42** (2005) 73 [arXiv:hep-lat/0410031].

[20] **ALPHA**, R. Frezzotti *et al.*, JHEP **08**, 058 (2001), [hep-lat/0101001].

[21] R. Frezzotti and G. C. Rossi, JHEP **08**, 007 (2004), [hep-lat/0306014].

[22] R. Frezzotti and G. C. Rossi, JHEP **10**, 070 (2004), [hep-lat/0407002].

[23] R. Frezzotti and G. C. Rossi, Nucl. Phys. Proc. Suppl. **128**, 193 (2004), [hep-lat/0311008].

[24] **ETMC**, R. Baron *et al.*, PoS **LATTICE 2010** (2010) 123. [arXiv:1101.0518].

[25] **ETMC**, R. Baron *et al.*, JHEP **1008**, 097 (2010). [arXiv:0911.5061].

[26] J. Gasser, H. Leutwyler, Phys. Lett. **B125** (1983) 325.

[27] G. Colangelo, S. Durr, C. Haefeli, Nucl. Phys. **B721** (2005) 136-174. [hep-lat/0503014].

[28] **FLAG**, G. Colangelo *et al.*, [arXiv:1011.4408].

[29] **ETMC**, V. Drach *et al.*, PoS **LATTICE 2010** (2010) 101. [arXiv:1012.3861].

[30] **ETMC**, S. Dinter *et al.*, PoS **LATTICE 2010**, 135 (2010). [arXiv:1101.5540].

[31] **ETMC**, B. Blossier *et al.*, Phys. Rev. **D82** (2010) 114513. [arXiv:1010.3659].

[32] S. Aoki, Phys. Rev. **D30** (1984) 2653.

[33] S. R. Sharpe, R. L. Singleton, Jr, Phys. Rev. **D58** (1998) 074501. [hep-lat/9804028].

[34] G. Münster, C. Schmidt, Europhys. Lett. **66** (2004) 652-656. [hep-lat/0311032].

[35] L. Scorzato, Eur. Phys. J. **C37** (2004) 445-455. [hep-lat/0407023].

[36] S. R. Sharpe, J. M. S. Wu, Phys. Rev. **D71** (2005) 074501. [hep-lat/0411021].

[37] R. Frezzotti, G.C. Rossi, PoS **LAT2007** (2007) 277. [arXiv:0710.2492].

[38] **ETMC**, P. Dimopoulos *et al.*, Phys. Rev. **D81** (2010) 034509. [arXiv:0908.0451].

[39] G. Colangelo, U. Wenger, J. M. S. Wu, Phys. Rev. **D82** (2010) 034502. [arXiv:1003.0847].

[40] O. Bär, Phys. Rev. **D82** (2010) 094505. [arXiv:1008.0784].

[41] L. Levkova, C. DeTar, [arXiv:1012.1837].

[42] **QCDSF-UKQCD**, W. Bietenholz *et al.*, PoS **LATTICE 2010** (2010) 122. [arXiv:1012.4371].

[43] **ETMC**, R. Baron *et al.*, Comput. Phys. Commun. **182** (2011) 299-316. [arXiv:1005.2042].

[44] **ETMC**, R. Baron *et al.*, PoS **LATTICE 2010**, 119 (2010) [arXiv:1009.2074].

[45] E. V. Luschevskaya, K. Cichy, [arXiv:1012.5047].

[46] K. Osterwalder, E. Seiler, Annals Phys. **110** (1978) 440.

[47] **ETMC**, M. Constantinou *et al.*, Phys. Rev. **D83** (2011) 014505. [arXiv:1009.5606].

[48] **ETMC**, P. Dimopoulos *et al.*, PoS **LATTICE 2010** (2010) 302. [arXiv:1012.3355].

[49] **ETMC**, F. Farchioni *et al.*, PoS **LATTICE 2010**, 128 (2010) [arXiv:1012.0200].

[50] S. Weinberg, Phys. Rev. **D8** (1973) 3497-3509.

[51] M. Lüscher *et al.*, Nucl. Phys. B **384** (1992) 168 [arXiv:hep-lat/9207009].

[52] G. Martinelli *et al.*, Nucl. Phys. **B445** (1995) 81-108. [hep-lat/9411010].

[53] Y. Aoki, PoS **LAT2009** (2009) 012. [arXiv:1005.2339].

[54] **PACS-CS**, S. Aoki *et al.*, JHEP **0910** (2009) 053. [arXiv:0906.3906].

[55] **PACS-CS**, S. Aoki *et al.*, JHEP **1008** (2010) 101. [arXiv:1006.1164].

[56] **BMW**, S. Durr *et al.*, [arXiv:1011.2711].

[57] **ETMC**, P. Dimopoulos *et al.*, PoS **LATTICE 2010** (2010) 235. [arXiv:1101.1877].

[58] **ETMC**, M. Constantinou *et al.*, JHEP **1008** (2010) 068. [arXiv:1004.1115].

[59] **ALPHA**, F. Tekin, R. Sommer, U. Wolff Nucl. Phys. **B840** (2010) 114-128. [arXiv:1006.0672].

[60] **ALPHA**, R. Sommer, F. Tekin, U. Wolff, PoS **LATTICE 2010** (2010) 241. [arXiv:1011.2332].

[61] P. Pérez-Rubio, S. Sint, PoS **LATTICE 2010** (2010) 236. [arXiv:1011.6580].